RESEARCH ARTICLE
doi: 10.2306/scienceasia1513-1874.2024.038

ScienceAsia 50 (2): 2024: ID 2024038: **1–10**

Role and mechanism of FDFT1 in regulating ferroptosis in colon cancer cells via the Nrf2/GPX4 pathway

Lin Mo[a], Xiaolin Wang[a], Xin Liu[a], Jian Gao[a], Chao Tan[b], Shunhai Jian[a,*]

[a] Department of Pathology, Basic Medicine and Forensic Medicine College, North Sichuan Medical College, Nanchong, Sichuan 637000 China

[b] Key Lab of Process Analysis and Control of Sichuan Universities, Yibin University, Yibin, Sichuan 644000 China

[*]Corresponding author, e-mail: Jianshunhai1972@163.com

Received 13 Apr 2023, Accepted 29 Nov 2023
Available online 3 May 2024

ABSTRACT: This study was to investigate the role of FDFT1 in colon cancer SW480 cells and its potential molecular mechanism. The survival prognosis of colon cancer patients was analyzed by TCGA database. FDFT1 mRNA expression in FHC, SW480, HCT116, and HT29 was analyzed by RT-qPCR. FDFT1 was overexpressed using pcDNA-FDFT1. Cell viability was measured by the CCK-8. Flow cytometry was used to detect cell death and ROS. Iron ion and LPO were also measured. The ultrastructure of SW480 cells was detected by TEM. The cellular behavior of SW480 was detected by wound healing and transwell invasion. GPX4 was detected by immunofluorescence. Western blot analysis was performed to detect FDFT1, Nrf2, HO-1, and GPX4. The results showed that FDFT1 was a positive factor in the prognosis of colon cancer. pcDNA-FDFT1 could lead to an increase in iron ion content and LPO in SW480. pcDNA-FDFT1 and erastin inhibited the proliferation of SW480 and affected ROS and mitochondrial structure. The ferroptosis inhibitor lip-1 inhibited the regulation of cell viability and ROS by pcDNA-FDFT1. pcDNA-FDFT1 and erastin inhibited the expression of Nrf2, HO-1, and GPX4. The Nrf2 agonist oltipraz reversed the effects of pcDNA-FDFT1 and restored the proliferation, migration, and invasive ability of SW480. The inhibition of Nrf2, HO-1, and GPX4 by pcDNA-FDFT1 was also up-regulated by oltipraz. In conclusion, up-regulation of FDFT1 induced iron death in SW480 cells through the Nrf2/GPX4 axis and was a positive factor in the prognosis of colon cancer.

KEYWORDS: FDFT1, ferroptosis, colon cancer, Nrf2/GPX4 pathway

INTRODUCTION

Colon cancer is a type of malignant tumor disease that occurs in the human digestive system [1, 2]. The incidence rate of this disease is rising year by year, and the prognosis is poor, endangering patients' lives [3]. In 2030, the number of new colorectal cancer cases is anticipated to exceed 2.2 million with 1.1 million deaths [4]. Stage diagnosis and radical resection can improve the prognosis of patients [5, 6]; however, patients with colon cancer lack symptoms in the early stages and once detected, they are usually already in the advanced stage of colon cancer, resulting in half of colon cancer patients being prone to recurrence and metastasis [7]. In view of this, early detection and primary prevention have become effective initiatives to significantly reduce mortality in patients with colon cancer [8]. Currently, clinical detection of colon cancer mainly relies on endoscopy and serum carcinoembryonic antigen screening, but its clinical application is limited by low sensitivity and specificity [9, 10]. As a result, the screening of novel molecular markers with high sensitivity and specificity and the elucidation of their molecular mechanisms in the development of colon cancer can significantly optimize the clinical treatment methods for the benefit of patients.

Ferroptosis has been widely studied and reported in the field of colon cancer, and iron, as an essential trace element, maintains the normal metabolic function of the body [11, 12]. Ferroptosis is a novel form of cell death distinct from autophagy and apoptosis and is an iron-dependent and reactive oxygen species (ROS)-dependent cell death [13]. It has been shown that ferroptosis can be triggered under a variety of physiological conditions and pathological stresses and plays a key role in tumorigenesis [14, 15]. Excess intracellular iron promotes the production of lipid peroxides, which in turn causes cell death [16]. Therefore, molecular prognostic models regulating ferroptosis-related genes are considered by many investigators as prognostic decisions for patients with colon cancer [17, 18]. Farnesyl-diphosphate farnesyltransferase1 (FDFT1) is a marker of ferroptosis in renal cell carcinoma [19].

In this study, we analyzed the molecular mechanism of ferroptosis-related genes in colon cancer using the TCGA colon cancer dataset and constructed a molecular prognostic model for colon cancer based on ferroptosis genes, aiming to provide a novel molecular prognostic marker for colon cancer and provide a reference basis for the diagnosis and prognostic assessment of colon cancer. The analysis identified FDFT1 as a positive factor in patient prognosis. FDFT1 is an important enzyme molecule in the endogenous synthesis pathway of cholesterol [20, 21]. Reports have shown that FDFT1 is aberrantly expressed in a variety of cancers, including liver, breast, prostate, and esophageal cancers, and it is considered a possible biomarker of cancer progression and a potential therapeutic target

[22]. However, the role of FDFT1 in the progression of colon cancer is unclear. This study will investigate the expression and survival of FDFT1 in colon cancer and its role in regulating the biological behavior of SW480 cells, providing a theoretical basis for the clinical prevention and treatment of colon cancer.

MATERIALS AND METHODS

Survival analysis in TCGA database

The RNA-seg data and corresponding clinical information of FDFT1 tumors were obtained from The Cancer Genome Atlas (TCGA) dataset (https://portal.gdc.com). Statistical analysis was performed using R software v4.0.3. A p value < 0.05 was considered statistically significant.

Cell culture and transfection

All cell lines were provided by the National Collection of Authenticated Cell Cultures, they were stored and cultured by the North Sichuan Medical College laboratory. SW480 (L15 medium, Biological Industries (BI), Israel), FHC (DMEM, BI), HCT116 (RPMI-1640, BI), and HT29 (RMPI-1640, BI) were cultured with the corresponding medium plus 10% FBS (BI) and grown in cell incubators (37 °C, 5% CO_2). The logarithmic growth phase cells were inoculated with the appropriate number of cells in a 6-well plate (Nest, China), and when their density grew to about 70%, pcDNA-FDFT1 (NM_001287742.2) and pcDNA-NC were transient transfected according to the instructions of ribo FECT™CP Transfection (RiboBio, Guangzhou, China). Plasmid Cloning Sites are *Hin*dIII (AAGCTT)-*Bam*HI (GGATCC). pcDNA-FDFT1 and pcDNA-NC were synthesized by GENERAL Biol (Anhui, China). In addition, erastin and oltipraz at appropriate concentrations and without cytotoxicity were selected for cellular experiments. The concentration of the ferroptosis inducer erastin (MedChemExpress, USA) was 10 μM. The concentration of the Nrf2 agonist oltipraz (MedChemExpress) was 40 μM. The cell culture medium was replaced 12 h after transfection, erastin and oltipraz were applied to SW480 cells for 24 h, and the cells were collected for subsequent detection.

CCK-8 assay for cell viability

SW480 cells were seeded into 96-well plates (Nest) and incubated at 37 °C in a 5% CO_2 incubator for 24 h. The plates were removed, and 10 μl of CCK-8 (Beyotime, China) reagent was added to each well and incubated for 1 h. The OD_{450} value of each well was detected by a microplate reader (Thermo Scientific, USA) at 450 nm.

qRT-PCR experiments

Total cellular RNA was extracted by Trizol Total RNA Extraction Kit (TaKaRa, Japan) and reverse transcribed into cDNA by Reverse Transcription Kit (TaKaRa). SYBR Premix Ex TaqTM II kit (TaKaRa) was used to detect the expression of FDFT1, and the results were analyzed by relative quantification according to the ddCT method. The average Ct value of each sample was calculated, and the relative mRNA expression level was expressed by $2^{-\mathrm{ddCt}}$. The primer sequences used in this study are as follows: FDFT1 Forward Primer 5′-AAGATGACATGACCATCAGTGT-3′, FDFT1 Reverse Primer 5′-CACTGTTTGGTATTTCTCAGCC-3′, β-actin Forward Primer 5′-CTGGTGCTGTCTGCGCTG-3′, and β-actin Reverse Primer 5′-CTGGGTTTCGTCTTTCTGG-3′. These primers were synthesized by Shanghai Sangon Biotech Co., Ltd (China).

Flow cytometry apoptosis assay

The logarithmic growth phase SW480 cells were inoculated in 12-well plates with 1×10^5 cells per well, and after the cells have fully adhered to the wall, transfection or drug administration intervention was performed. After 48 h, all cells in the 6-well plates were collected, washed with PBS to remove the background, resuspended in 100 μl 1 × Binding Buffer, incubated with FITC-AnnexinV and PE-PI dual fluorescent probes (Yeasen, China) for 15 min at room temperature and protected from light, and immediately detected on the machine, using the flow-through FITC/PI channel to detect the proportion of apoptotic cells by Flow Cytometry (Beckman Coulter, USA).

Flow cytometry for ROS

SW480 cells were seeded in 6-well plates, and 1×10^6 cells from each group were washed twice in PBS. The cells were probe-loaded, prepared as 500 μl suspension cells containing 5 mol/l DCFH-DA (MCE), reacted for 30 min in the dark at 37 °C, and washed twice with PBS. The FITC channel was chosen to examine the changes in ROS in various groups. The optical density of the cells detected by the FITC channel was used to count the changes in ROS.

TEM assay

SW480 cells were fixed in 5% glutaraldehyde (Aladdin, China) for 5 h at 4 °C before being washed 3 times for 10 min each with neutral phosphate buffer. SW480 cells were then fixed in 0.1 mol/l osmium acid (Aladdin) for 3 h before being washed 3 times in phosphate buffer for 10 min each time. The gradient dehydration was then performed for 15 min at 50%, 70%, 80%, 90%, 95%, and 100% ethanol (Aladdin). The resin was impregnated, embedded, polymerized, and double-stained with uranium lead before being photographed using Transmission Electron Microscope (TEM, JEOL, Japan).

Immunofluorescence detection of GPX4 expression in SW480

SW480 was fixed in paraformaldehyde, washed, sealed, and incubated overnight with GPX4 antibody

(1:500, Abcam, UK). SW480 samples were washed 4 times with PBS containing Tween, 5 min each time. After 1 h of incubation with the fluorescent secondary antibody (Univbio, China), the SW480 sample was sealed with a DAPI-containing fluorescent quenching mountant (Yeasen). OlympusBX51 fluorescence microscope (Olympus, Japan) was used to observe and photograph the slices.

Wound healing assay to detect the healing ability of SW480 cells

SW480 cells were inoculated in 24-well plates (Nest) at a density of 2×10^5 cells/well, and when cell fusion reached 90% or higher, a vertical scratch was made in the center of the plate with a 10 µl gun tip, and the suspended cells were washed 3 times with PBS to remove the scratch, before being placed in an incubator (37 °C, 5% CO_2) for further incubation. The scratch distance was calculated using ImageJ software after photographing the scratch area at 0 and 24 h after the scratch.

Transwell assay for migratory capacity of SW480 cells

SW480 cells were digested, centrifuged, and resuspended in serum-free medium and then inoculated at a cell density of 5×10^5 cells/well in the Transwell upper chamber (Nest) at 200 µl per well, and 600 µl of medium containing 20% serum was added to the lower chamber. Then, Transwell chambers were incubated in an incubator (37 °C, 5% CO_2) for 48 h, and the upper chamber was removed and repeatedly washed with PBS, fixed with 4% paraformaldehyde for 30 min, stained with crystal violet for 5 min, and wiped off the unmigrated cells in the upper chamber with a cotton swab dipped in PBS. Five fields of view (200×) were randomly selected to observe and count the number of cells crossing the chambers.

Western blot analysis

Western blot analysis was performed for protein expression level detection. Log phase SW480 cells were inoculated in 6-well plates, and the cells were collected after 48 h of culture. Then, 300 µl of RIPA cell lysis solution (containing 1% mercaptoethanol, Yeasen) was added to each well, lysed in the ice bath for 5 min, and then processed by ultrasonic disintegrator for 10 min. Then, all lysed cell samples were heated at 100 °C for 10 min. The 30 µg samples were loaded onto SDS vertical gel (8%–10%) for electrophoretic separation, and the completed separated proteins were transferred (220V) onto PVDF membranes. After sealing the PVDF membrane with 5% milk powder for 1 h, FDFT1 antibody (1:1000), Nrf2 antibody (1:500), HO-1 (heme oxygenase 1) antibody (1:500), and GPX4 (Glutathione Peroxidase 4) antibody (1:500) were added and incubated overnight at 4 °C in a shaker. After washing the membrane, the secondary antibody dilution (1:7000) was added and incubated for 1 h at room temperature, and the membrane was washed 4 times (15 min each time) in PBST before developing on a chemiluminescence instrument to pick up the target proteins and analyze the protein grayscale values of each group of strips. All antibodies were from Abcam.

Detection of iron ions and LPO

Iron ion levels in SW480 cells were determined using an iron ion detection kit (ml095089, Shanghai Enzyme Biotechnology Co., Ltd., China) according to the manufacturer's instructions. The reagents used in the iron ion detection process do not contain iron ion chelating agents. Lipid peroxide (LPO) reacts at 45 °C for 60 min. One molecule of LPO reacts with 2 molecules of chromogenic reagent (A106-1, NanJing JianCheng Bioengineering Institute, China) to produce a stable chromophore with a maximum absorption peak at 586 nm.

Statistical analysis

The experimental data were statistically analyzed using Prism8, and the results of each experiment were repeated 3 times independently. The experimental data were expressed as mean ± standard error (SEM). A one-way ANOVA analysis was used for comparison between multiple groups, and a t-test was used for comparison between the 2 groups. $p < 0.05$ was statistically significant.

RESULTS

Expression and prognostic analysis of FDFT1 in colon cancer

To further investigate the relationship between the expression level of FDFT1 and colon cancer, we performed a consistent cluster analysis on the data from all 455 colon cancer patient samples in the TCGA cohort. In the TCGA database, there were 228 patients with high FDFT1 expression and 227 patients with low FDFT1 expression (Fig. 1A). Kaplan-Meier analysis showed a significant difference in overall survival (OS) between the 2 patient populations (Fig. 1B). These results suggest that FDFT1 is a positive factor for patient prognosis.

Expression of FDFT1 in colon cancer cell lines and colonic mucosal epithelial cell lines

The normal colonic mucosal epithelial cell line FHC was selected as a control, and the expression of FDFT1 mRNA in colonic carcinoma cell lines SW480, HCT116, and HT29 were compared. As shown in Fig. 2A, compared with FHC, FDFT1 was highly expressed in HCT116 and HT29, and FDFT1 had the lowest expression level in SW480, so SW480 was selected as the research object. Under the premise that FDFT1 is an oncogene, pcDNA-FDFT1 was constructed to

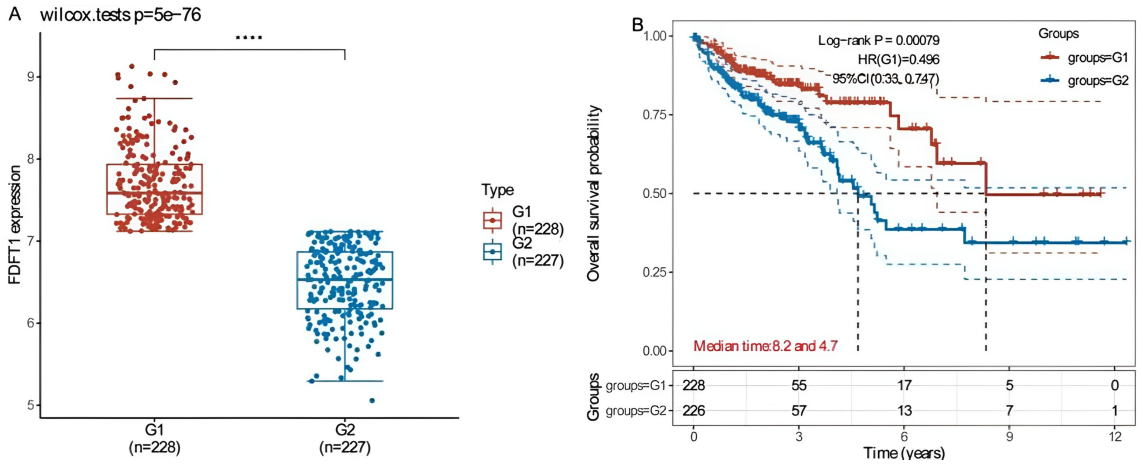

Fig. 1 OS analysis of overall survival differences between patients with FDFT1 high (G1) and low (G2) expression in colon cancer. (A): FDFT1 differential expression. (B): Kaplan-Meier survival curves. Data are mean ± SEM, **** $p < 0.001$.

overexpress FDFT1. As shown in Fig. 2B, pcDNA-NC did not affect FDFT1 mRNA compared with the control, while pcDNA-FDFT1 significantly up-regulated FDFT1 mRNA. In addition, pcDNA-NC did not affect the expression of FDFT1 protein compared with the control group, while pcDNA-FDFT1 significantly up-regulated the expression of FDFT1 protein (Fig. 2C and D). As shown in Fig. 2E, compared with pcDNA-NC, the cell viability of SW480, HCT116, and HT29 decreased, with the most decrease in cell viability of SW480. In addition, compared with pcDNA-NC, pcDNA-FDFT1 increased the contents of iron ions and LPO in SW480 cells (Fig. 2F and G). Compared with the control group, the level of FDFT1 mRNA increased after erastin treatment (Fig. 2H). The above experimental results indicate that stable overexpression of FDFT1 can be constructed in SW480 cells.

Effect of FDFT1 expression on ferroptosis in colon cancer cells

To further explore the effect of FDFT1 on SW480 proliferation, pcDNA-FDFT1 in combination with the ferroptosis inducer erastin was used to observe the proliferative capacity of SW480 cells. In comparison with pcDNA-NC, pcDNA-FDFT1 and erastin inhibited the proliferation of SW480. The lowest OD value of cells in the combined group of pcDNA-FDFT1 and erastin implied the weakest cell proliferation (Fig. 3A). Similarly, compared with pcDNA-NC, pcDNA-FDFT1 and erastin induced SW480 cell death, and pcDNA-FDFT1 combined with erastin resulted in the most dead cells (Fig. 3B and C). ROS is a factor closely associated with ferroptosis. In comparison with pcDNA-NC, pcDNA-FDFT1 and erastin induced the level of ROS, and the highest level of ROS was observed in the combined group of pcDNA-FDFT1 and erastin (Fig. 3D and E).

In addition, pcDNA-FDFT1 and erastin inhibited the expression of Nrf2 and HO-1 compared with pcDNA-NC, and pcDNA-FDFT1 and erastin combined with Nrf2 and HO-1 had the lowest expression levels. Similar to the immunofluorescence results, GPX4 protein levels were highest in the pcDNA-NC group. pcDNA-FDFT1 and erastin down-regulated GPX4 expression, and with the combination of both, GPX4 was most significantly down-regulated (Fig. 3F–I). These results suggest that Nrf2/GPX4 is involved in the regulation of SW480 ferroptosis by FDFT1.

Effect of FDFT1 on the Nrf2/GPX4 pathway

GPX4, a representative protein of ferroptosis, can characterize SW480 ferroptosis. In comparison with pcDNA-NC, pcDNA-FDFT1 and erastin inhibited GPX4 expression, and the lowest GPX4 expression level was found in the combined group of pcDNA-FDFT1 and erastin (Fig. 4A and B). Compared with pcDNA-NC, the morphological structure of the cells appeared abnormal after erastin induction. The chromatin in the nucleus was uniformly distributed, mainly euchromatin, and heterochromatin was attached under the nuclear membrane, but the perinuclear gap was widened. Some mitochondria in the cytoplasm became smaller, the membrane density was increased, and the cristae were broken. The rough endoplasmic reticulum was dilated; more autophagy and a few vacuoles appeared in the cytoplasm. Moreover, pcDNA-FDFT1 was able to counteract some of the damage of SW480 by erastin (Fig. 4C). As shown in Fig. 4D, compared with pcDNA-NC, the cell viability of the pcDNA-FDFT1 group decreased. Compared with the pcDNA-FDFT1 group, the cell viability increased after the ferroptosis inhibitor liproxstatin-1 (lip-1) was added. In addition, compared with pcDNA-NC, ROS increased in the pcDNA-FDFT1 group; compared with the pcDNA-

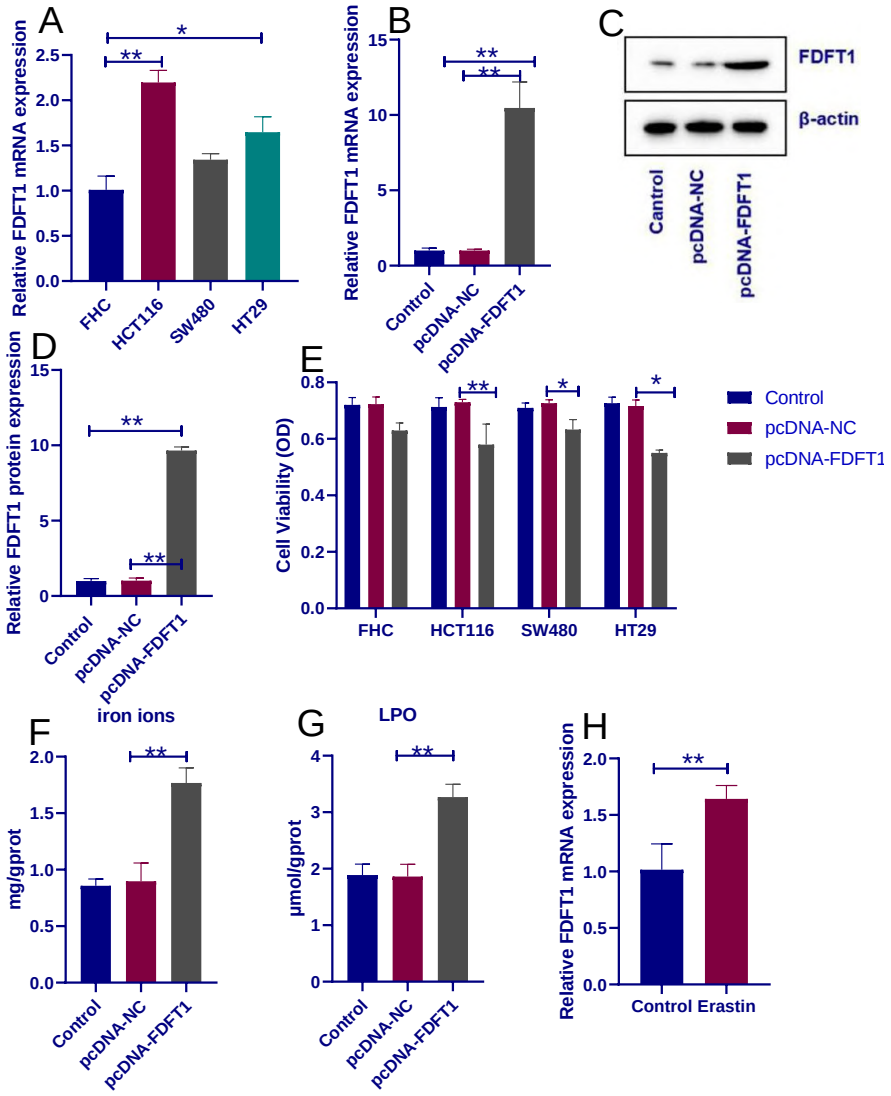

Fig. 2 Construction of colon cell lines overexpressing FDFT1. (A): Expression of FDFT1 in colon epithelial cells (FHC) and colon cancer cells (SW480, HCT116, and HT29). (B): Induction of FDFT1 mRNA by pcDNA-FDFT1 in SW480. (C) and (D): Upregulation of FDFT1 protein expression by pcDNA-FDFT1 in SW480. (E): Effect of pcDNA-FDFT1 on the viability of FHC, SW480, HCT116, and HT29 cells. (F): Effect of pcDNA-FDFT1 on iron ion content. (G): Effect of pcDNA-FDFT1 on LPO. (H): Effect of erastin (10 μM) on FDFT1 mRNA. Data are mean ± SEM, * $p < 0.05$, ** $p < 0.01$.

FDFT1 group, cellular ROS weakened after the action of ferroptosis inhibitor lip-1 (Fig. 4E and F).

Effect of FDFT1 regulation of Nrf2/GPX4 on the behavior of SW480 cells

The Nrf2 agonist oltipraz was combined with pcDNA-FDFT1 to observe changes in SW480 proliferation, apoptosis, migration, and invasion. As shown in Fig. 5A, compared with pcDNA-NC, pcDNA-FDFT1 inhibited the proliferation of SW480, and oltipraz had no significant effect on the proliferation of SW480; compared with pcDNA-FDFT1, oltipraz reversed the inhibitory effect of pcDNA-FDFT1. Flow cytometry results showed that oltipraz had no significant effect on SW480 death compared to pcDNA-NC and that oltipraz combined with pcDNA-FDFT1 had reduced SW480 cell death compared to pcDNA-FDFT1 (Fig. 5B and C). As shown in Fig. 5D and E, there was no difference in the migration distance of SW480 at 24 h between pcDNA-NC and oltipraz groups. Compared with pcDNA-FDFT1, the migration distance of SW480 at 24 h was reduced in the combination group of oltipraz and pcDNA-FDFT1. Next, a transwell cell migration assay was performed. Compared with the pcDNA-NC, pcDNA-FDFT1 reduced the migratory capacity of SW480, and oltipraz could inhibit the effect of pcDNA-

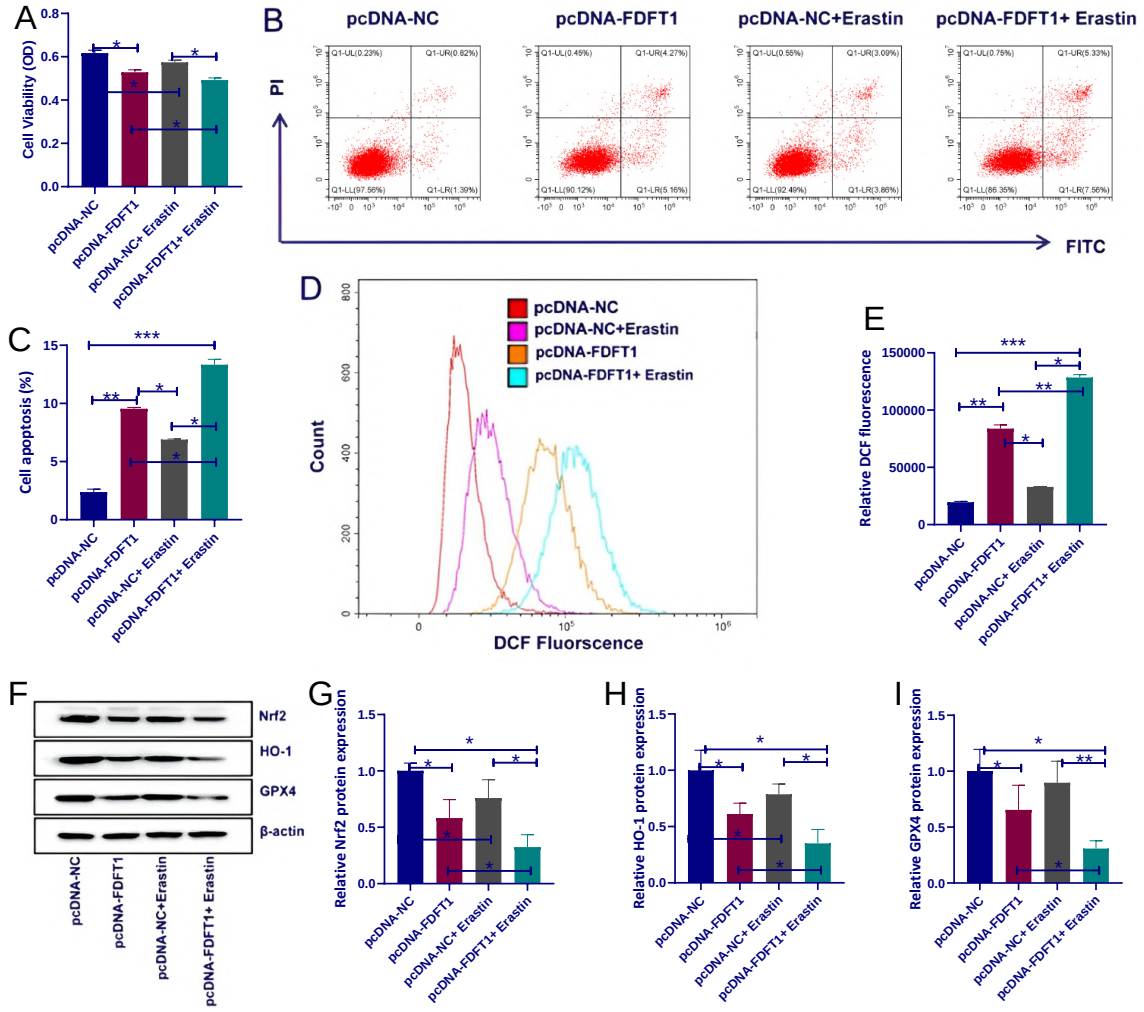

Fig. 3 pcDNA-FDFT1 and erastin affecting SW480 ferroptosis. (A): Proliferation ability of SW480 by CCK-8. (B) and (C): pcDNA-FDFT1 and erastin inducing SW480 death. (D) and (E): pcDNA-FDFT1 and erastin affecting SW480 ROS. (F–I): Western blot detection of Nrf2, HO-1, and GPX4. Data are mean ± SEM, * $p < 0.05$, ** $p < 0.01$, *** $p < 0.001$.

FDFT1 (Fig. 5F and G). As for proteins Nrf2, HO-1, and GPX4, pcDNA-FDFT1 down-regulated the expression of Nrf2, HO-1, and GPX4, and oltipraz could reverse the effect of pcDNA-FDFT1 to some extent (Fig. 5H–K). Based on the above experimental results, it was found that up-regulated FDFT1 can affect Nrf2, HO-1, and GPX4 to promote ferroptosis in SW480 cells (Fig. 6).

DISCUSSION

With the continuous improvement of medical technology, the average life expectancy of human beings has been extended; however, the incidence of malignant tumors has been increasing, among which colon cancer has become an important risk factor affecting human life and health [1, 2]. According to the International Agency for Research on Cancer GLOBOCAN 2020 data, approximately 940,000 people die from colon cancer worldwide [23]. Because of the extremely insidious development of colon cancer, the early diagnosis rate is low, and most patients are already in the middle and late stages when diagnosed [24].

Tumorigenesis and progression are jointly regulated by many factors, and these regulatory factors can regulate the expression of oncogenes and play a role in promoting or inhibiting tumor progression [25]. FDFT1 is a membrane-associated enzyme located at the branching point of the mevalonate pathway [26]. Alterations in FDFT1 expression are usually observed in cancer, including regulation of non-coding RNAs, and overexpression of FDFT1 suppresses ovarian cancer by decreasing miR-4425 [27]. Due to the important role of FDFT1 in tumor progression, it is expected to be a target for anticancer therapy [28]. FDFT1 is located on chromosome 8p23.1 (Chromosome 8-NC_000008.11), and FDFT1 is associated with a positive prognosis in ovarian cancer [27]. FDFT1 has been

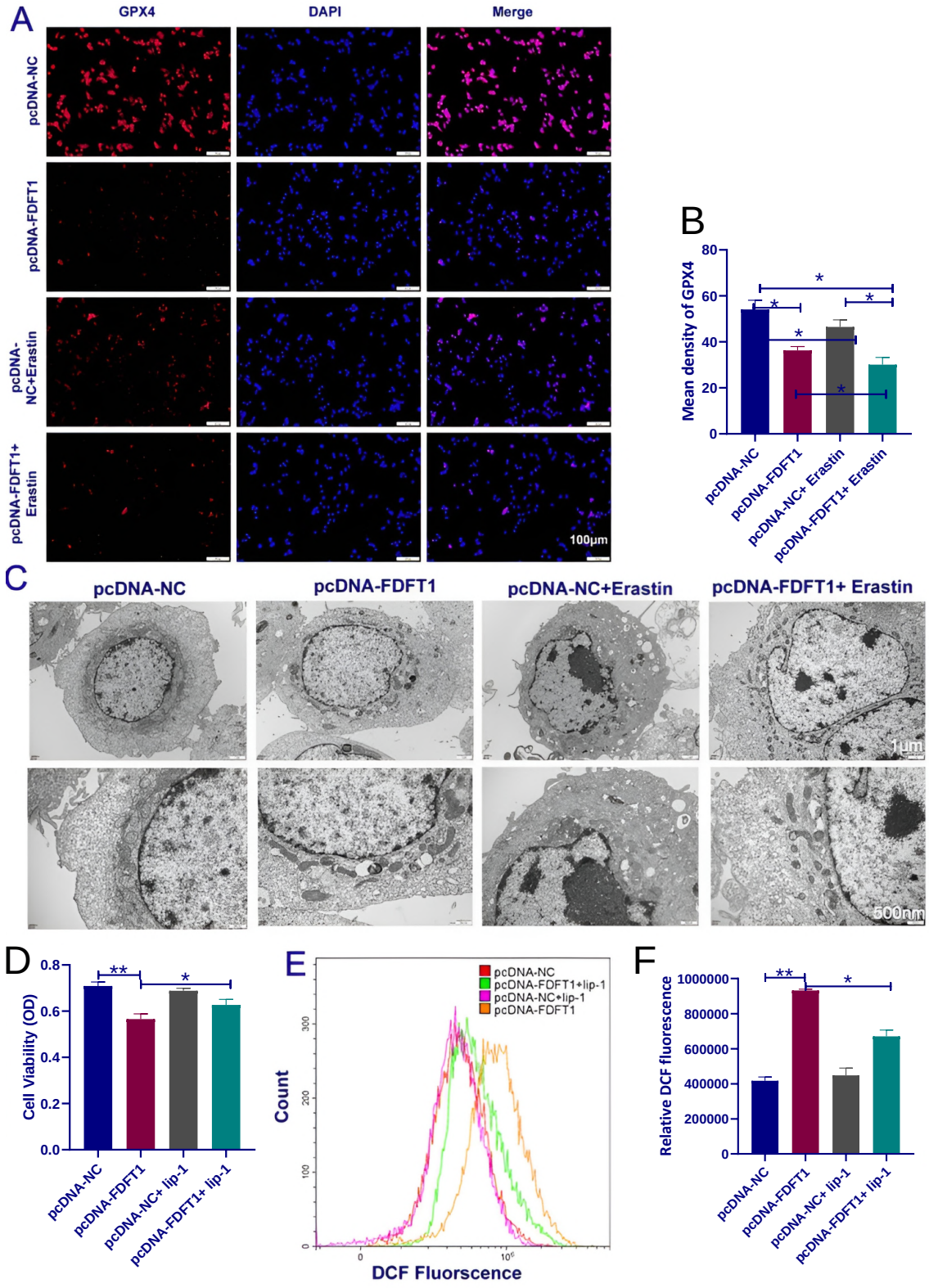

Fig. 4 Mechanisms by which FDFT1 affects ferroptosis in SW480. (A) and (B): Immunofluorescence for GPX4. (C): Transmission electron microscope observation of changes in cellular ferroptosis characteristics. (D): Effect of ferroptosis inhibitor lip-1 (1 μM) and pcDNA-FDFT1 on cell viability. (E): Effect of ferroptosis inhibitor lip-1 and pcDNA-FDFT1 on ROS. Data are mean ± SEM, * $p < 0.05$, ** $p < 0.01$.

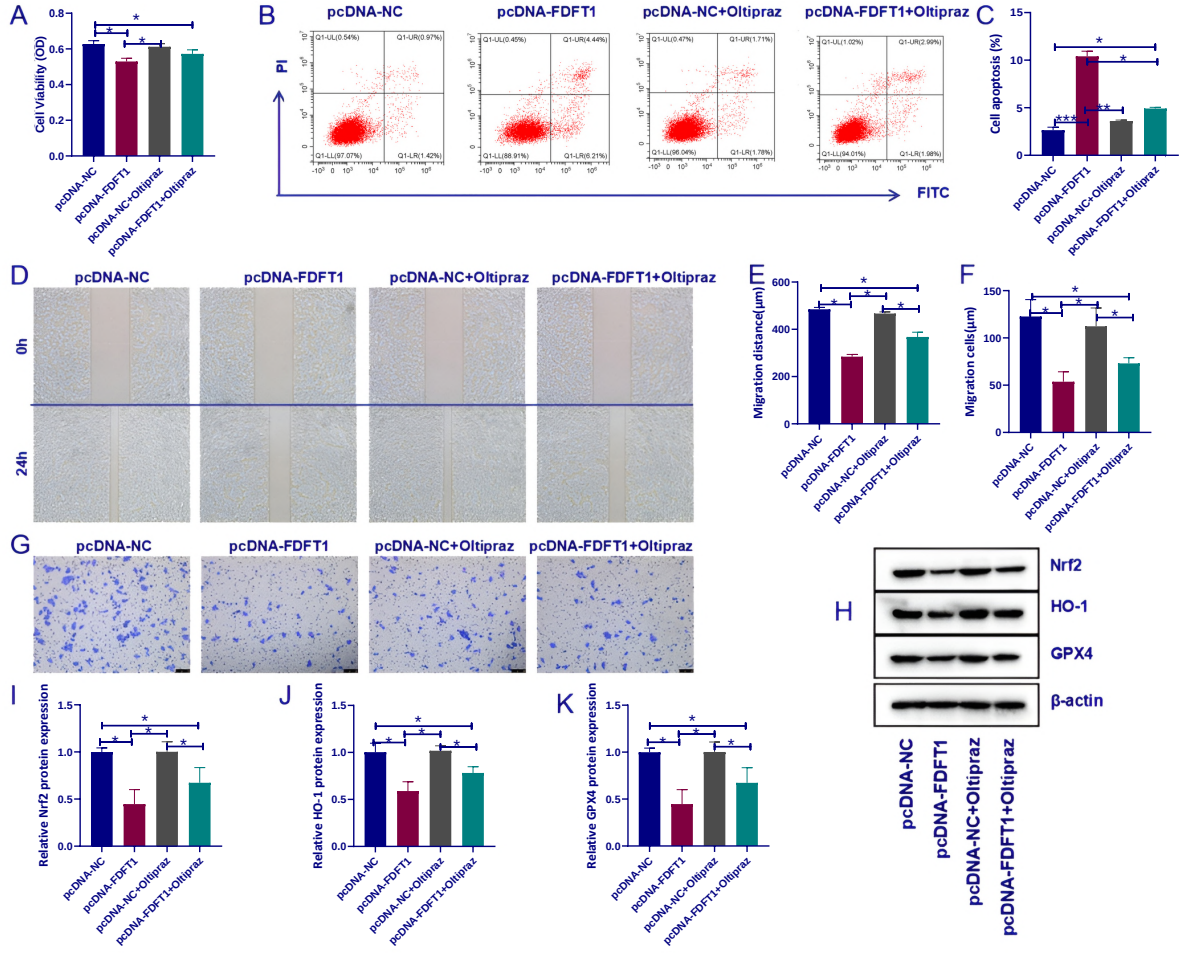

Fig. 5 FDFT1 regulating Nrf2/GPX4 on the proliferation, apoptosis, migration, and invasion of colon cancer cells. (A): CCK-8 detecting the proliferation ability of SW480. (B) and (C): Effects of pcDNA-FDFT1 and oltipraz on SW480 mortality. (D) and (E): Wound healing assay of SW480 influenced by pcDNA-FDFT1and oltipraz. (F) and (G): Transwell migration of SW480 influenced by pcDNA-FDFT1and oltipraz. (H–K): Western blot detection of Nrf2, HO-1, and GPX4. Data are mean ± SEM, * $p < 0.05$, ** $p < 0.01$, *** $p < 0.001$.

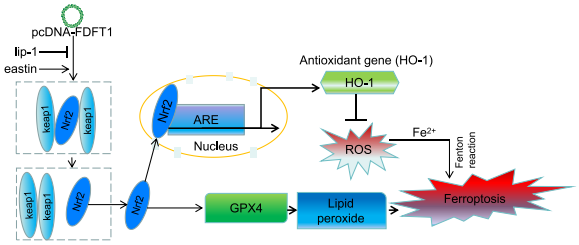

Fig. 6 Schematic summarizing mechanism of FDFT1 in regulating ferroptosis in this study.

reported to be related to the growth and metabolism of bladder cancer [29], and FDFT1 is also a marker of ferroptosis in renal cell carcinoma [19]. In this study, the expression of FDFT1 in colon cancer and the impact on prognosis were reported for the first time by bioinformatics analysis based on the TCGA database. The results showed that high expression of FDFT1 was a positive factor in the prognosis of colon cancer patients.

With the identification of FDFT1 as a positive prognostic factor for colon cancer, the expression of FDFT1 mRNA in colon cancer cells SW480, HCT116, and HT29 was analyzed, and the lower expressed SW480 was selected for transfection with pcDNA-FDFT1 to construct FDFT1 overexpression cells. Both FDFT1 protein and mRNA were significantly up-regulated by pcDNA-FDFT1 in this study. In addition, metastasis and invasion of cancer cells are typical features of tumor cells. Tumor metastasis is a complex process involving cell migration, invasion, and adhesion [30, 31]. Among them, migration is a key aspect of

cancer cell invasion and metastasis [32]. The pcDNA-FDFT1-induced cell lines had diminished migratory and invasive abilities, indicating that FDFT1 expression could inhibit the metastasis of colon cancer cells. Also, cell proliferation assays showed that pcDNA-FDFT1 could significantly inhibit the growth of SW480. These experimental results are consistent with the results obtained from the TCGA database analysis that FDFT1 inhibits the growth of colon cancer and responds positively to the prognosis of patients.

Previous studies have shown the identification of FDFT1 as a potential biomarker associated with ferroptosis in renal cell carcinoma [19]. In the field of colon cancer, activation of the AMPK/mTOR/p70S6k signaling pathway inhibits SLC7A11 expression and reduces cystine and GSH levels to inhibit colon cancer cell proliferation [33]. Induction of HO-1 expression increases intracellular free iron concentration and improves ferroptosis sensitivity of colon cancer cells [34]. In this study, both flow cytometry and CCK-8 results indicated that erastin induced ferroptosis in SW480 cells. Erastin is the first small molecule reported to kill rat sarcoma (Ras) cells and simultaneously up-regulate ferrous ions in tumor cells, ultimately producing large amounts of reactive oxygen species (ROS) to induce cell death [35, 36]. We found that pcDNA-FDFT1 and erastin had similar effects and were able to induce ROS production. These imply that the inhibition of SW480 by FDFT1 involves ferroptosis.

Ferroptosis is a form of cell death that exhibits iron-dependent, intracellular accumulation of lipid-reactive oxygen species [37]. Self-morphology is mainly characterized by characteristic morphological features such as blistering of the plasma membrane, increased cytoplasmic as well as lipid ROS, normal nuclei, reduced or absent mitochondrial cristae, mitochondrial crinkling, and increased mitochondrial membrane density [38]. Biometabolically, intracellular redox homeostasis is disrupted, antioxidant capacity is reduced, and reactive oxygen species are elevated [16]. GPX4 is a selenoprotein that specifically and efficiently scavenges phospholipid peroxide, thereby inhibiting the onset of ferroptosis [39]. GPX4 degrades iron overload-induced hydrogen peroxide and other small molecule peroxides in cells and can prevent ferroptosis caused by massive accumulation of ROS [40]. The expression of GPX4 was affected by FDFT1 in this study, and mitochondria were also deformed by the action of pcDNA-FDFT1. In addition, Nrf2 was also influenced by FDFT1, with more ROS under Nrf2 inhibition conditions. The study by Sun et al [41] identified the Keap1-Nrf2 signaling pathway that up-regulates target genes downstream of Nrf2 involved in iron and ROS metabolism such as quinone oxidoreductase 1 (NQO1), heme oxygenase 1 (HO-1), and ferritin heavy chain-1 (FTH1), thereby enhancing the ferroptosis resistance of sorafenib. All these aforementioned studies can demonstrate that FDFT1 regulates ferroptosis in SW480 cells through Nrf2.

CONCLUSION

In summary, the present study was validated by comprehensive bioinformatics analysis and molecular and cellular levels and found that overexpression of FDFT1 could promote ferroptosis to inhibit cell migration and invasion, which may provide a new idea for the diagnosis and treatment of patients with colon cancer.

Appendix A. Supplementary data

The datasets used or analyzed during the current study are available from the corresponding author on reasonable request.

Acknowledgements: Funding: (1) Key Lab of Process Analysis and Control of Sichuan Universities (No.2020002); (2) The Science and Technology Project of Municipal School Strategic Cooperation, Nanchong (22SXQT0328).

REFERENCES

1. Tie J, Cohen JD, Lahouel K, Lo SN, Wang Y, Kosmider S, Wong R, Shapiro J, et al (2022) Circulating tumor DNA analysis guiding adjuvant therapy in stage II colon cancer. *N Engl J Med* **386**, 2261–2272.
2. Fabregas JC, Ramnaraign B, George TJ (2022) Clinical updates for colon cancer care in 2022. *Clin Colorectal Cancer* **21**, 198–203.
3. Liu H, Ma L, Wang L, Yang Y (2019) MicroRNA-937 is overexpressed and predicts poor prognosis in patients with colon cancer. *Diagn Pathol* **14**, 136.
4. Ahmed M (2020) Colon cancer: A clinician's perspective in 2019. *Gastroenterology Res* **13**, 1–10.
5. Zhou R, Zhang J, Zeng D, Sun H, Rong X, Shi M, Bin J, Liao Y, et al (2019) Immune cell infiltration as a biomarker for the diagnosis and prognosis of stage I–III colon cancer. *Cancer Immunol Immunother* **68**, 433–442.
6. Khan FA, Aldahhan R, Almohazey D (2021) Impact of gold nanoparticles on colon cancer treatment and diagnosis. *Nanomedicine (Lond)* **16**, 779–782.
7. Su Y, Tian X, Gao R, Guo W, Chen C, Chen C, Jia D, Li H, et al (2022) Colon cancer diagnosis and staging classification based on machine learning and bioinformatics analysis. *Comput Biol Med* **145**, 105409.
8. Ruan H, Leibowitz BJ, Zhang L, Yu J (2020) Immunogenic cell death in colon cancer prevention and therapy. *Mol Carcinog* **59**, 783–793.
9. Mody K, Bekaii-Saab T (2018) Clinical trials and progress in metastatic colon cancer. *Surg Oncol Clin N Am* **27**, 349–365.
10. Bashiri M, Akçalı D, Coşkun D, Cindoruk M, Dikmen A, Çifdalöz BU (2018) Evaluation of pain and patient satisfaction by music therapy in patients with endoscopy-/colonoscopy. *Turk J Gastroenterol* **29**, 574–579.
11. Wang Y, Xia HB, Chen ZM, Meng L, Xu AM (2021) Identification of a ferroptosis-related gene signature predictive model in colon cancer. *World J Surg Oncol* **19**, 135.
12. Zhu J, Kong W, Xie Z (2021) Expression and prognostic characteristics of ferroptosis-related genes in colon cancer. *Int J Mol Sci* **22**, 5652.

13. Mou Y, Wang J, Wu J, He D, Zhang C, Duan C, Li B (2019) Ferroptosis, a new form of cell death: opportunities and challenges in cancer. *J Hematol Oncol* **12**, 34.
14. Deng Z, Manz DH, Torti SV, Torti FM (2017) Iron-responsive element-binding protein 2 plays an essential role in regulating prostate cancer cell growth. *Oncotarget* **8**, 82231–82243.
15. Torti SV, Manz DH, Paul BT, Blanchette-Farra N, Torti FM (2018) Iron and cancer. *Annu Rev Nutr* **38**, 97–125.
16. Florean C, Song S, Dicato M, Diederich M (2019) Redox biology of regulated cell death in cancer: A focus on necroptosis and ferroptosis. *Free Radic Biol Med* **134**, 177–189.
17. Chen Z, Wu T, Yan Z, Zhang M (2021) Identification and validation of an 11-ferroptosis related gene signature and its correlation with immune checkpoint molecules in glioma. *Front Cell Dev Biol* **9**, 652599.
18. Yao X, Chen B, Wang M, Zhang S, He B, Shi Z, Deng T, Bao W, et al (2022) Exploration and validation of a novel ferroptosis-related gene signature predicting the prognosis of intrahepatic cholangiocarcinoma. *Acta Biochim Biophys Sin* **54**, 1376–1385.
19. Huang R, Zhang C, Wang X, Zou X, Xiang Z, Wang Z, Gui B, Lin T, et al (2022) Identification of FDFT1 as a potential biomarker associated with ferroptosis in ccRCC. *Cancer Med* **11**, 3993–4004.
20. Ha NT, Lee CH (2020) Roles of farnesyl-diphosphate farnesyltransferase 1 in tumour and tumour microenvironments. *Cells* **9**, 2352.
21. Do R, Kiss RS, Gaudet D, Engert JC (2009) Squalene synthase: a critical enzyme in the cholesterol biosynthesis pathway. *Clin Genet* **75**, 19–29.
22. Tüzmen Ş, Hostetter G, Watanabe A, Ekmekçi C, Carrigan PE, Shechter I, Kallioniemi O, Miller LJ, et al (2019) Characterization of farnesyl diphosphate farnesyl transferase 1 (FDFT1) expression in cancer. *Per Med* **16**, 51–65.
23. Sung H, Ferlay J, Siegel RL, Laversanne M, Soerjomataram I, Jemal A, Bray F (2021) Global cancer statistics 2020: GLOBOCAN estimates of incidence and mortality worldwide for 36 cancers in 185 countries. *CA Cancer J Clin* **71**, 209–249.
24. Tran Q, Warren JL, Barrett MJ, Annett D, Marth M, Cress RD, Deapen D, Glaser SL, et al (2020) An evaluation of the utility of big data to supplement cancer treatment information: Linkage between IQVIA pharmacy database and the surveillance, epidemiology, and end results program. *J Natl Cancer Inst Monogr* **2020**, 72–81.
25. Zeng M, Zhu L, Li L, Kang C (2017) miR-378 suppresses the proliferation, migration and invasion of colon cancer cells by inhibiting SDAD1. *Cell Mol Biol Lett* **22**, 12.
26. Griffin S, Healey GD, Sheldon IM (2018) Isoprenoids increase bovine endometrial stromal cell tolerance to the cholesterol-dependent cytolysin from *Trueperella pyogenes*. *Biol Reprod* **99**, 749–760.
27. Lu J, Zhou Y, Zheng C, Chen L, Tuo X, Chen H, Xue M, Chen Q, et al (2020) 20(S)-Rg3 upregulates FDFT1 via reducing miR-4425 to inhibit ovarian cancer progression. *Arch Biochem Biophys* **693**, 108569.
28. Wang Q, Karvelsson ST, Johannsson F, Vilhjalmsson AI, Hagen L, de Miranda Fonseca D, Sharma A, Slupphaug G, et al (2022) UDP-glucose dehydrogenase expression is upregulated following EMT and differentially affects intracellular glycerophosphocholine and acetylaspartate levels in breast mesenchymal cell lines. *Mol Oncol* **16**, 1816–1840.
29. Kanmalar M, Abdul Sani SF, Kamri N, Said N, Jamil A, Kuppusamy S, Mun KS, Bradley DA (2022) Raman spectroscopy biochemical characterisation of bladder cancer cisplatin resistance regulated by FDFT1: a review. *Cell Mol Biol Lett* **27**, 9.
30. Jiang WG, Hiscox S, Singhrao SK, Puntis MC, Nakamura T, Mansel RE, Hallett MB (1995) Induction of tyrosine phosphorylation and translocation of ezrin by hepatocyte growth factor/scatter factor. *Biochem Biophys Res Commun* **217**, 1062–1069.
31. Zhang Q, Bi R, Bao X, Xu X, Fang D, Jiang L (2022) MYT1L promotes the migration and invasion of glioma cells through activation of Notch signaling pathway. *ScienceAsia* **48**, 711–717.
32. Kim EK, Yun SJ, Ha JM, Kim YW, Jin IH, Yun J, Shin HK, Song SH, et al (2011) Selective activation of Akt1 by mammalian target of rapamycin complex 2 regulates cancer cell migration, invasion, and metastasis. *Oncogene* **30**, 2954–2963.
33. Zhang L, Liu W, Liu F, Wang Q, Song M, Yu Q, Tang K, Teng T, et al (2020) IMCA induces ferroptosis mediated by SLC7A11 through the AMPK/mTOR pathway in colorectal cancer. *Oxid Med Cell Longev* **2020**, 1675613.
34. Malfa GA, Tomasello B, Acquaviva R, Genovese C, La Mantia A, Cammarata FP, Ragusa M, Renis M, et al (2019) *Betula etnensis* Raf. (Betulaceae) extract induced HO-1 expression and ferroptosis cell death in human colon cancer cells. *Int J Mol Sci* **20**, 2723.
35. Lei G, Zhuang L, Gan B (2022) Targeting ferroptosis as a vulnerability in cancer. *Nat Rev Cancer* **22**, 381–396.
36. Dixon SJ, Lemberg KM, Lamprecht MR, Skouta R, Zaitsev EM, Gleason CE, Patel DN, Bauer AJ, et al (2012) Ferroptosis: an iron-dependent form of nonapoptotic cell death. *Cell* **149**, 1060–1072.
37. Zhao L, Zhou X, Xie F, Zhang L, Yan H, Huang J, Zhang C, Zhou F, et al (2022) Ferroptosis in cancer and cancer immunotherapy. *Cancer Commun (Lond)* **42**, 88–116.
38. You H, Wang L, Bu F, Meng H, Huang C, Fang G, Li J (2022) Ferroptosis: shedding light on mechanisms and therapeutic opportunities in liver diseases. *Cells* **11**, 3301.
39. Capelletti MM, Manceau H, Puy H, Peoc'h K (2020) Ferroptosis in liver diseases: An overview. *Int J Mol Sci* **21**, 4908.
40. Ye Z, Liu W, Zhuo Q, Hu Q, Liu M, Sun Q, Zhang Z, Fan G, et al (2020) Ferroptosis: Final destination for cancer? *Cell Prolif* **53**, e12761.
41. Sun X, Ou Z, Chen R, Niu X, Chen D, Kang R, Tang D (2016) Activation of the p62-Keap1-NRF2 pathway protects against ferroptosis in hepatocellular carcinoma cells. *Hepatology* **63**, 173–184.